

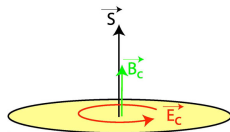
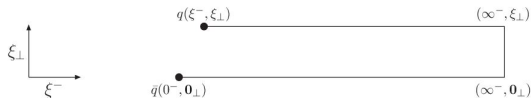
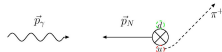
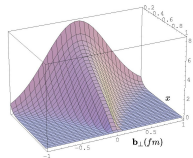
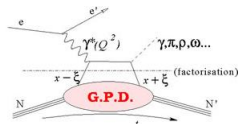
Transverse Force Tomography

Matthias Burkardt

*New Mexico State University

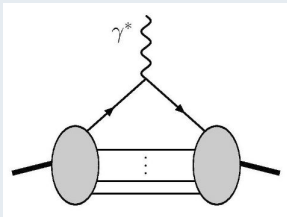
September 24, 2018

- **GPDs** \rightarrow **3D imaging** of the nucleon
 - twist-3 PDFs $g_2(x) \rightarrow \perp$ **force**
 - \hookrightarrow twist-3 GPDs \rightarrow **\perp force tomography**
- Motivation: why twist-3 GPDs
- twist-3 GPD $G_2^q \rightarrow L^q$
 - twist 3 PDF $g_2(x) \rightarrow \perp$ force
 - twist 2 GPDs $\rightarrow \perp$ imaging (of quark densities)
 - \hookrightarrow twist 3 GPDs $\rightarrow \perp$ **imaging of \perp forces**
- Summary
 - Outlook



form factor

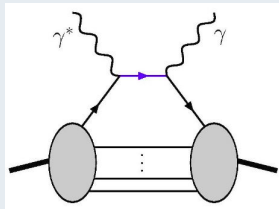
- electron hits nucleon & nucleon remains intact



- study amplitude that nucleon remains intact as function of momentum transfer $\rightarrow F(q^2)$
 - $F(q^2) = \int dx GPD(x, q^2)$
- \rightarrow GPDs provide momentum dissected form factors

Compton scattering

- electron hits nucleon, nucleon remains intact & photon gets emitted



- study both energy & q^2 dependence
- \rightarrow additional information about momentum fraction x of active quark
- \rightarrow generalized parton distributions $GPD(x, q^2)$

MB, PRD62, 071503 (2000)

- form factors: $\overleftrightarrow{FT} \rho(\vec{r})$
 - $GPDs(x, \vec{\Delta})$: form factor for quarks with momentum fraction x
- ↪ suitable FT of $GPDs$ should provide spatial distribution of quarks with momentum fraction x

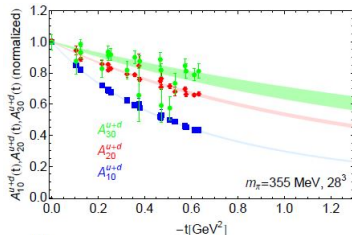
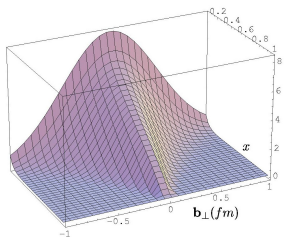
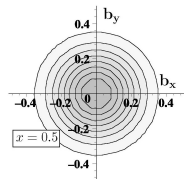
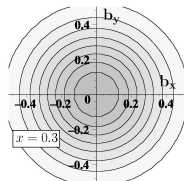
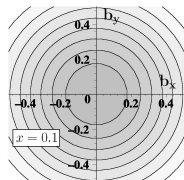
Impact Parameter Dependent Quark Distributions

$$q(x, \mathbf{b}_\perp) = \int \frac{d^2 \Delta_\perp}{(2\pi)^2} GPD(x, -\Delta_\perp^2) e^{-i\mathbf{b}_\perp \cdot \Delta_\perp}$$

$q(x, \mathbf{b}_\perp)$ = parton distribution as a function of the separation \mathbf{b}_\perp from the transverse center of momentum $\mathbf{R}_\perp \equiv \sum_{i \in q, g} \mathbf{r}_{\perp, i} x_i$

- probabilistic interpretation!
 - no relativistic corrections: Galilean subgroup! (MB,2000)
- ↪ corollary: interpretation of 2d-FT of $F_1(Q^2)$ as charge density in transverse plane also free from relativistic corrections (MB,2003;G.A.Miller, 2007)

$q(x, \mathbf{b}_\perp)$ for unpol. p



unpolarized proton

- $q(x, \mathbf{b}_\perp) = \int \frac{d^2 \Delta_\perp}{(2\pi)^2} H(x, 0, -\Delta_\perp^2) e^{-i\mathbf{b}_\perp \cdot \Delta_\perp}$
 - $F_1(-\Delta_\perp^2) = \int dx H(x, 0, -\Delta_\perp^2)$
 - x = momentum fraction of the quark
 - \mathbf{b}_\perp relative to \perp center of momentum
 - small x : large 'meson cloud' (\rightarrow C. Weiss)
 - larger x : compact 'valence core'
 - $x \rightarrow 1$: active quark becomes center of momentum
- $\hookrightarrow \vec{b}_\perp \rightarrow 0$ (narrow distribution) for $x \rightarrow 1$

2. Quantum Chromodynamics: The Fundamental Description of the Heart of Visible Matter

represents the first fruit of more than a decade of effort in this direction.

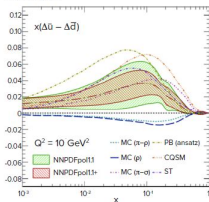


Figure 2.4: The difference between the Δ_0 and Δ_1 spin functions as extracted from the NNPDF global analysis. The green (red) band shows the proton (first separated) uncertainties from analysis of the RHIC W data set. Various model calculations are also shown.

A Multidimensional View of Nucleon Structure

"With 3D projection, we will be entering a new age. Something which was never technically possible before: a stunning visual experience which 'turbocharges' the viewing." This quotation from film director J. Cameron could just as well describe developments over the last decade or so in hadron physics, in which a multidimensional description of nucleon structure is emerging that is providing profound new insights. Form factors tell us about the distribution of charge and magnetization but contain no direct dynamical information. PDFs allow us to access information on the underlying quarks and their longitudinal momentum but tell us nothing about spatial locations. It has now been established, however, that both form factors and PDFs are special cases of a more general class of distribution functions that merge spatial and dynamic information. Through appropriate measurements, it is becoming possible to construct "pictures" of the nucleon that were never before possible.

3D Spatial Maps of the Nucleon: GPDs

Some of the important new tools for describing hadrons are Generalized Parton Distributions (GPDs). GPDs can be investigated through the analysis of *hard exclusive* processes, processes where the target is probed

by high-energy particles and is left intact beyond the production of one or two additional particles.

Two processes are recognized as the most powerful processes for accessing GPDs: deeply virtual Compton scattering (DVCS) and deeply virtual meson production (DVMP) where a photon or a meson, respectively, is produced.

One striking way to use GPDs to enhance our understanding of hadronic structure is to use them to construct what we might call 3D spatial maps (see Sidebar 2.2). For a particular value of the momentum fraction x , we can construct a spatial map of where the quarks reside. With the JLab 12-GeV Upgrade, the valence quarks will be accurately mapped.

GPDs can also be used to evaluate the total angular momentum associated with different types of quarks, using what is known as the Ji Sum Rule. By combining with other existing data, one can directly access quark orbital angular momentum. The worldwide DVCS experimental program, including that at Jefferson Lab with a 6-GeV electron beam and at HERMES with 27-GeV electron and positron beams, has already provided constraints (albeit model dependent) on the total angular momentum of the u and d quarks. These constraints can also be compared with calculations from LQCD. Upcoming 12-GeV experiments at JLab and COMPASS-II experiments at CERN will provide dramatically improved precision. A suite of DVCS and DVMP experiments is planned in Hall B with CLAS12; in Hall A with HRS and existing calorimeters; and in Hall C with HMS, the new SHMS, and the Neutral Particle Spectrometer (NPS). These new data will transform the current picture of hadronic structure.

3D Momentum Maps of the Nucleon: TMDs

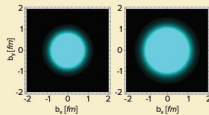
Other important new tools for describing nucleon structure are transverse momentum dependent distribution functions (TMDs). These contain information on both the longitudinal and transverse momentum of the quarks (and gluons) inside a fast moving nucleon. TMDs link the transverse motion of the quarks with their spin and/or the spin of the parent proton and are, thus, sensitive to orbital angular momentum. Experimentally, these functions can be investigated in proton-proton collisions, in inclusive production of lepton pairs in Drell-Yan processes, and in *semi-inclusive deep inelastic scattering* (SIDIS), where one measures the scattered electron and one more meson (typically a pion or kaon) in the DIS process.

Sidebar 2.2: The First 3D Pictures of the Nucleon

A computed tomography (CT) scan can help physicians pinpoint minute cancer tumors, diagnose tiny broken bones, and spot the early signs of osteoporosis. Now physicists are using the principles behind the procedure to peer at the inner workings of the proton. This breakthrough is made possible by a relatively new concept in nuclear physics called generalized parton distributions.

An intense beam of high-energy electrons can be used as a microscope to look inside the proton. The high energies tend to disrupt the proton, so one or more new particles are produced. Physicists often disregarded what happened to the debris and measured only the energy and position of the scattered electron. This method is called inclusive deep inelastic scattering and has revealed the most basic grains of matter, the quarks. However, it has a limitation: it can only give a one-dimensional image of the substructure of the proton because it essentially measures the momentum of the quarks along the direction of the incident electron beam. To provide the three-dimensional (3D) picture, we need instead to measure all the particles in the debris. This way, we can construct a 3D image of the proton as successive spatial quark distributions in planes perpendicular to its motion for slices in the quark's momentum, just like a 3D image of the human body can be built from successive planar views.

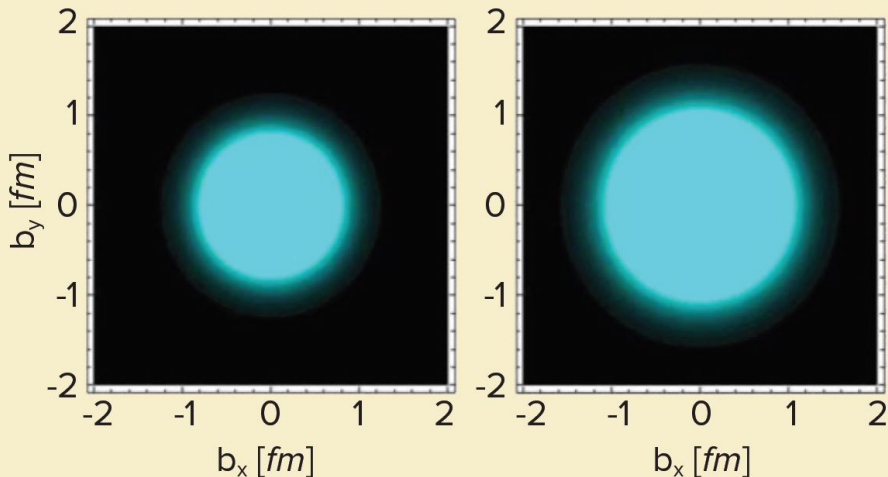
An electron can scatter from a proton in many ways. We are interested in those collisions where a high-energy electron strikes an individual quark inside the proton, giving the quark a very large amount of extra energy. This quark then quickly gets rid of its excess energy, for instance, by emitting a high-energy photon. The quark does not change identity and remains part of the intact target proton. This specific process is called deeply virtual Compton scattering (DVCS). For the experiment to work, the scientists need to measure the speed, position, and energy of the electron that bounced off the quark, of the photon emitted by the quark, and of the reassembled proton. From this information the 3D picture of the proton can be constructed.



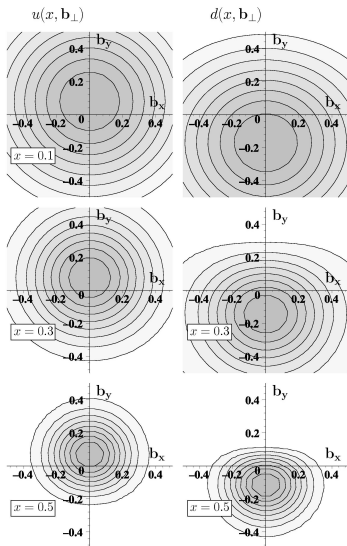
The first 3D slices of the proton: the spatial charge densities of the proton in a plane (b_x, b_y) positioned at two different values of the quark's longitudinal momentum x : 0.25 (left) and 0.99 (right).

Very recently, using the DVCS data collected with the CLAS detector at JLab and the HERMES detector at DESY/Germany, the first nearly model-independent images of the proton started to appear. The result of this work is illustrated in the figure, where the probabilities for the quarks to reside at various places inside the proton are shown at two different values of its longitudinal momentum x ($x = 0.25$ left and $x = 0.99$ right). This is analogous to the "orbital" clouds used to depict the likely position of electrons in various energy levels inside atoms. The first 3D pictures of the proton indicate that when the longitudinal momentum x of the quark decreases, the radius of the proton increases.

The broader implications of these results are that we now have methods to fill in the information needed to extract 3D views of the proton. Physicists worldwide are working toward this goal, and the technique pioneered here will be applied with Jefferson Lab's CEBAF accelerator at 12 GeV for (valence) quarks and, later, with a future EIC for gluons and sea quarks.



The first 3D views of the proton: the spatial charge densities of the proton in a plane (b_x, b_y) positioned at two different values of the quark's longitudinal momentum x : 0.25 (left) and 0.09 (right).



proton polarized in $+\hat{x}$ direction

no axial symmetry!

$$q(x, \mathbf{b}_\perp) = \int \frac{d^2 \Delta_\perp}{(2\pi)^2} H_q(x, -\Delta_\perp^2) e^{-i\mathbf{b}_\perp \cdot \Delta_\perp} \\ - \frac{1}{2M} \frac{\partial}{\partial b_y} \int \frac{d^2 \Delta_\perp}{(2\pi)^2} E_q(x, -\Delta_\perp^2) e^{-i\mathbf{b}_\perp \cdot \Delta_\perp}$$

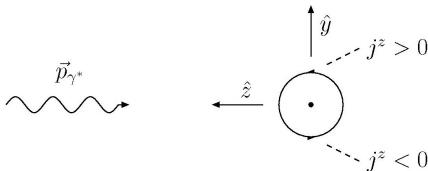
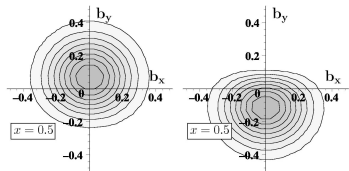
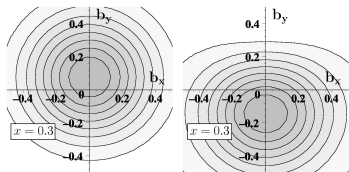
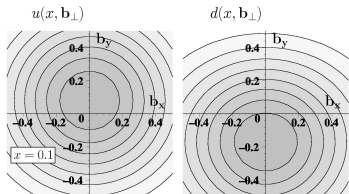
Physics: relevant density in DIS is

$j^+ \equiv j^0 + j^3$ and left-right asymmetry from j^3

intuitive explanation

- moving Dirac particle with anomalous magnetic moment has electric dipole moment \perp to \vec{p} and \perp magnetic moment

$\hookrightarrow \gamma^*$ 'sees' flavor dipole moment of oncoming nucleon

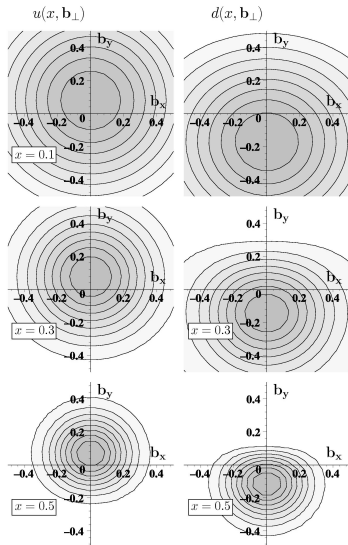


proton polarized in $+\hat{x}$ direction

no axial symmetry!

$$q(x, \mathbf{b}_\perp) = \int \frac{d^2 \Delta_\perp}{(2\pi)^2} H_q(x, -\Delta_\perp^2) e^{-i\mathbf{b}_\perp \cdot \Delta_\perp} - \frac{1}{2M} \frac{\partial}{\partial b_y} \int \frac{d^2 \Delta_\perp}{(2\pi)^2} E_q(x, -\Delta_\perp^2) e^{-i\mathbf{b}_\perp \cdot \Delta_\perp}$$

Physics: relevant density in DIS is $j^+ \equiv j^0 + j^3$ and left-right asymmetry from j^3



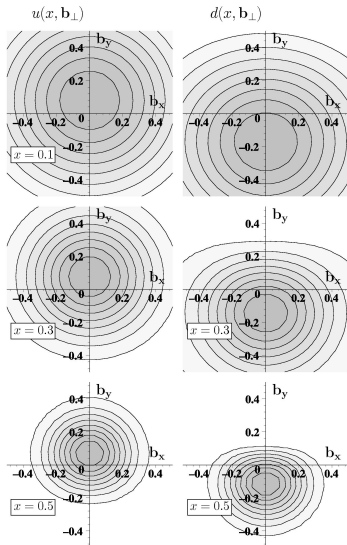
proton polarized in $+\hat{x}$ direction

$$q(x, \mathbf{b}_\perp) = \int \frac{d^2 \Delta_\perp}{(2\pi)^2} H_q(x, -\Delta_\perp^2) e^{-i\mathbf{b}_\perp \cdot \Delta_\perp} \\ - \frac{1}{2M} \frac{\partial}{\partial b_y} \int \frac{d^2 \Delta_\perp}{(2\pi)^2} E_q(x, -\Delta_\perp^2) e^{-i\mathbf{b}_\perp \cdot \Delta_\perp}$$

sign & magnitude of the average shift

model-independently related to p/n
anomalous magnetic moments:

$$\langle b_y^q \rangle \equiv \int dx \int d^2 b_\perp q(x, \mathbf{b}_\perp) b_y \\ = \frac{1}{2M} \int dx E_q(x, 0) = \frac{\kappa_q}{2M}$$



sign & magnitude of the average shift

model-independently related to p/n
anomalous magnetic moments:

$$\begin{aligned}\langle b_y^q \rangle &\equiv \int dx \int d^2 b_\perp q(x, \mathbf{b}_\perp) b_y \\ &= \frac{1}{2M} \int dx E_q(x, 0) = \frac{\kappa_q}{2M}\end{aligned}$$

$$\kappa^P = 1.913 = \frac{2}{3}\kappa_u^P - \frac{1}{3}\kappa_d^P + \dots$$

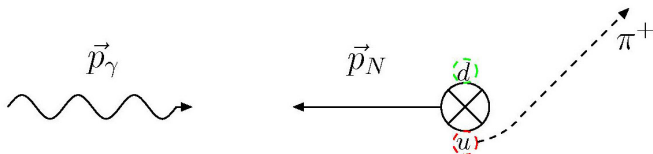
- u -quarks: $\kappa_u^P = 2\kappa_p + \kappa_n = 1.673$

↪ shift in $+\hat{y}$ direction

- d -quarks: $\kappa_d^P = 2\kappa_n + \kappa_p = -2.033$

↪ shift in $-\hat{y}$ direction

- $\langle b_y^q \rangle = \mathcal{O}(\pm 0.2 \text{ fm})$!!!!

example: $\gamma p \rightarrow \pi X$ 

- u, d distributions in \perp polarized proton have left-right asymmetry in \perp position space (T-even!); sign “determined” by κ_u & κ_d
- attractive final state interaction (FSI) deflects active quark towards the center of momentum
- \hookrightarrow FSI translates position space distortion (before the quark is knocked out) in $+\hat{y}$ -direction into momentum asymmetry that favors $-\hat{y}$ direction \rightarrow **chromodynamic lensing**

 \Rightarrow $\kappa_p, \kappa_n \longleftrightarrow$ sign of SSA!!!!!!! (MB,2004)

- confirmed by HERMES & COMPASS data

$d_2 \leftrightarrow$ average \perp force on quark in DIS from \perp pol target

polarized DIS:

$$\bullet \sigma_{LL} \propto g_1 - \frac{2Mx}{\nu} g_2 \qquad \bullet \sigma_{LT} \propto g_T \equiv g_1 + g_2$$

\hookrightarrow 'clean' separation between g_2 and $\frac{1}{Q^2}$ corrections to g_1

$$\bullet g_2 = g_2^{WW} + \bar{g}_2 \text{ with } g_2^{WW}(x) \equiv -g_1(x) + \int_x^1 \frac{dy}{y} g_1(y)$$

$$d_2 \equiv 3 \int dx x^2 \bar{g}_2(x) = \frac{1}{2MP^{+2}S_x} \langle P, S | \bar{q}(0) \gamma^+ g F^{+y}(0) q(0) | P, S \rangle$$

color Lorentz Force on ejected quark (MB, PRD 88 (2013) 114502)

$$\sqrt{2}F^{+y} = F^{0y} + F^{zy} = -E^y + B^x = -\left(\vec{E} + \vec{v} \times \vec{B}\right)^y \text{ for } \vec{v} = (0, 0, -1)$$

matrix element defining $d_2 \leftrightarrow$ 1st integration point in QS-integral

$d_2 \Rightarrow \perp$ force \leftrightarrow QS-integral $\Rightarrow \perp$ impulse

sign of d_2

$$\bullet \perp \text{ deformation of } q(x, \mathbf{b}_\perp)$$

\hookrightarrow sign of d_2^q : opposite Sivers

magnitude of d_2

$$\bullet \langle F^y \rangle = -2M^2 d_2 = -10 \frac{\text{GeV}}{f_m} d_2$$

$$\bullet |\langle F^y \rangle| \ll \sigma \approx 1 \frac{\text{GeV}}{f_m} \Rightarrow d_2 = \mathcal{O}(0.01)$$

$d_2 \leftrightarrow$ average \perp force on quark in DIS from \perp pol target

polarized DIS:

$$\bullet \sigma_{LL} \propto g_1 - \frac{2Mx}{\nu} g_2 \qquad \bullet \sigma_{LT} \propto g_T \equiv g_1 + g_2$$

\hookrightarrow 'clean' separation between g_2 and $\frac{1}{Q^2}$ corrections to g_1

$$\bullet g_2 = g_2^{WW} + \bar{g}_2 \text{ with } g_2^{WW}(x) \equiv -g_1(x) + \int_x^1 \frac{dy}{y} g_1(y)$$

$$d_2 \equiv 3 \int dx x^2 \bar{g}_2(x) = \frac{1}{2MP^{+2}S_x} \langle P, S | \bar{q}(0) \gamma^+ g F^{+y}(0) q(0) | P, S \rangle$$

color Lorentz Force on ejected quark (MB, PRD 88 (2013) 114502)

$$\sqrt{2}F^{+y} = F^{0y} + F^{zy} = -E^y + B^x = -\left(\vec{E} + \vec{v} \times \vec{B}\right)^y \text{ for } \vec{v} = (0, 0, -1)$$

sign of d_2

$$\bullet \perp \text{ deformation of } q(x, \mathbf{b}_\perp)$$

\hookrightarrow sign of d_2^q : opposite Sivers

magnitude of d_2

$$\bullet \langle F^y \rangle = -2M^2 d_2 = -10 \frac{\text{GeV}}{fm} d_2$$

$$\bullet |\langle F^y \rangle| \ll \sigma \approx 1 \frac{\text{GeV}}{fm} \Rightarrow d_2 = \mathcal{O}(0.01)$$

consistent with experiment (JLab, SLAC), model calculations (Weiss), and lattice QCD calculations (Göckeler et al., 2005)

chirally even spin-dependent twist-3 PDF $g_2(x)$ MB, PRD 88 (2013) 114502

- $\int dx x^2 g_2(x) \Rightarrow \perp$ force on unpolarized quark in \perp polarized target
- \hookrightarrow ‘Sivers force’

scalar twist-3 PDF $e(x)$ MB, PRD 88 (2013) 114502

- $\int dx x^2 e(x) \Rightarrow \perp$ force on \perp polarized quark in unpolarized target
- \hookrightarrow ‘Boer-Mulders force’

chirally odd spin-dependent twist-3 PDF $h_2(x)$ M.Abdallah & MB, PRD94 (2016) 094040

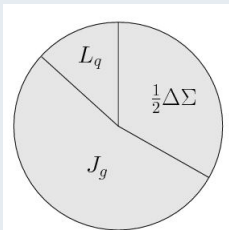
- $\int dx x^2 h_2(x) = 0$
- $\hookrightarrow \perp$ force on \perp pol. quark in long. pol. target vanishes due to parity
- $\int dx x^3 h_2(x) \Rightarrow$ long. gradient of \perp force on \perp polarized quark in long. polarized target
- \hookrightarrow chirally odd ‘wormgear force’

force distributions

F.Aslan & MB: work in progress

- use FT of twist-3 GPDs to map these forces in the \perp plane

Ji decomposition



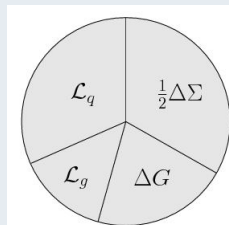
'pizza tre stagioni'

$$\frac{1}{2} = \sum_q \left(\frac{1}{2} \Delta q + L_q \right) + J_g$$

$$\vec{L}_q = \vec{r} \times (\vec{p} - g\vec{A})$$

- manifestly gauge inv. & local
- DVCS \rightarrow GPDs $\rightarrow L^q$

Jaffe-Manohar decomposition



'pizza quattro stagioni'

$$\frac{1}{2} = \sum_q \left(\frac{1}{2} \Delta q + \mathcal{L}_q \right) + \Delta G + \mathcal{L}_g$$

$$\vec{\mathcal{L}}_q = \vec{r} \times \vec{p}$$

- manifestly gauge inv. \rightarrow nonlocal
- $\vec{p} \overleftarrow{p} \rightarrow \Delta G \rightarrow \mathcal{L} \equiv \sum_{i \in q,g} \mathcal{L}^i$

How large is difference $\mathcal{L}_q - L_q$ in QCD and what does it represent?

Ji

$$\frac{1}{2} = \sum_q \frac{1}{2} \Delta q + L_q + J_g$$

$$L_q = \vec{r} \times (\vec{p} - g\vec{A})$$

Jaffe-Manohar

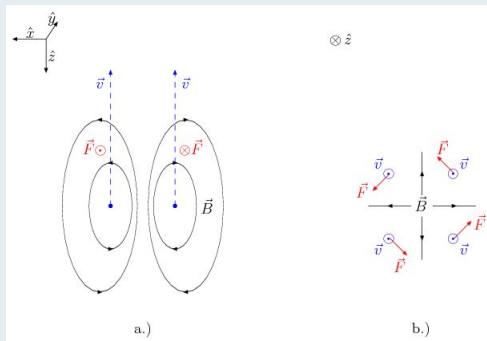
$$\frac{1}{2} = \sum_q \frac{1}{2} \Delta q + \mathcal{L}_q + \Delta G + \mathcal{L}_g$$

$$\vec{\mathcal{L}}^q = \vec{r} \times \vec{p}$$

difference $\mathcal{L}^q - L^q$ (MB, PRD 88 (2013) 014014)

$\mathcal{L}^q - L^q = \Delta L_{FSI}^q = \text{change in OAM as quark leaves nucleon}$

example: torque in magnetic dipole field



difference $\mathcal{L}^q - L^q$

$\mathcal{L}_{JM}^q - L_{Ji}^q = \Delta L_{FSI}^q =$ change in OAM as quark leaves nucleon

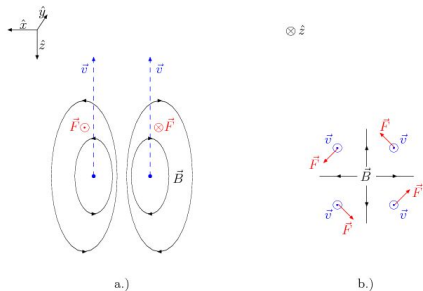
$$\mathcal{L}_{JM}^q - L_{Ji}^q = -g \int d^3x \langle P, S | \bar{q}(\vec{x}) \gamma^+ [\vec{x} \times \int_{x^-}^{\infty} dr^- F^{+\perp}(r^-, \mathbf{x}_{\perp})]^z q(\vec{x}) | P, S \rangle$$

e^+ moving through dipole field of e^-

- consider e^- polarized in $+\hat{z}$ direction
- $\hookrightarrow \vec{\mu}$ in $-\hat{z}$ direction (Figure)
- e^+ moves in $-\hat{z}$ direction
- \hookrightarrow net torque **negative**

sign of $\mathcal{L}^q - L^q$ in QCD

- color electric force between two q in nucleon attractive
- \hookrightarrow same as in positronium
- spectator spins positively correlated with nucleon spin
- \hookrightarrow expect $\mathcal{L}^q - L^q < 0$ in nucleon



difference $\mathcal{L}^q - L^q$

$\mathcal{L}_{JM}^q - L_{Ji}^q = \Delta L_{FSI}^q =$ change in OAM as quark leaves nucleon

$$\mathcal{L}_{JM}^q - L_{Ji}^q = -g \int d^3x \langle P, S | \bar{q}(\vec{x}) \gamma^+ [\vec{x} \times \int_{x^-}^{\infty} dr^- F^{+\perp}(r^-, \mathbf{x}_{\perp})]^z q(\vec{x}) | P, S \rangle$$

e^+ moving through dipole field of e^-

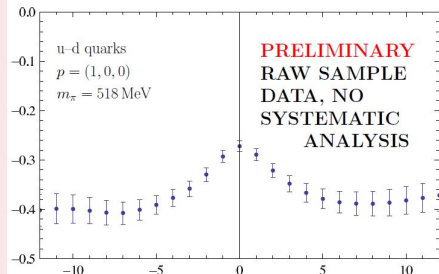
- consider e^- polarized in $+\hat{z}$ direction
- $\hookrightarrow \vec{\mu}$ in $-\hat{z}$ direction (Figure)
- e^+ moves in $-\hat{z}$ direction
- \hookrightarrow net torque **negative**

sign of $\mathcal{L}^q - L^q$ in QCD

- color electric force between two q in nucleon attractive
- \hookrightarrow same as in positronium
- spectator spins positively correlated with nucleon spin
- \hookrightarrow expect $\mathcal{L}^q - L^q < 0$ in nucleon

lattice QCD (M.Engelhardt)

- L_{staple} vs. staple length
- $\hookrightarrow L_{Ji}^q$ for length = 0
- $\hookrightarrow \mathcal{L}_{JM}^q$ for length $\rightarrow \infty$



- shown $L_{staple}^u - L_{staple}^d$
- similar result for each ΔL_{FSI}^q

twist-3 GPDs (Meissner, Metz, Schlegel) – example $\Gamma = \gamma^x \gamma_5$

$$\int dz^- e^{ixz^-} \bar{p}^+ \langle P' | \bar{q}(z^-/2) \gamma^x \gamma_5 q(-z^-/2) | p \rangle = \frac{-i}{2(P^+)^2} \times$$

$$\bar{u}(p') \left[i\sigma^{+y} H'_{2T} + \frac{\gamma^+ \Delta^i - \Delta^+ \gamma^y}{2M} E'_{2T} + \frac{P^+ \Delta^y - \Delta^+ P^y}{M^2} \tilde{H}'_{2T} + \frac{\gamma^+ P^y - P^+ \gamma^y}{2M} \tilde{E}'_{2T} \right] u(p)$$

- $H'_{2T}(x, \xi, t)$ etc. all twist 3 GPDs
- similar for $\gamma = \mathbf{1}, \gamma_5, \gamma^\perp, \sigma^{ij} \gamma_5, \sigma^{+-} \gamma_5$ (16 GPDs)

physics of twist-3 GPDs

- x^2 -moment $\Rightarrow \langle p' | \bar{q}(0) \gamma^x \gamma_5 \overset{\leftrightarrow}{D}_-^2 q(0) | p \rangle \rightsquigarrow \langle p' | \bar{q}(0) \gamma^+ F^{+y} q(0) | p \rangle +$
twist-2
- $\Rightarrow x^2$ -moment of twist-3 GPDs \rightsquigarrow matrix elements of 'force operator' $\bar{q} \gamma^+ F^{+y} q$
- $\Rightarrow \perp$ momentum transfer \rightsquigarrow spatial resolution
- \Rightarrow transverse force tomography (\perp vectorfields of \perp forces)
- $\Gamma = \gamma^x \gamma_5$: force in \hat{y} direction for unpolarized quarks

⊥ localized state

$$|\mathbf{R}_\perp = 0, p^+, \Lambda\rangle \equiv \mathcal{N} \int d^2\mathbf{p}_\perp |\mathbf{p}_\perp, p^+, \Lambda\rangle$$

⊥ force distribution (unpolarized quarks)

$$\begin{aligned} F_{\Lambda'\Lambda}^i(\mathbf{b}_\perp) &\equiv \langle \mathbf{R}_\perp = 0, p^+, \Lambda' | \bar{q}(\mathbf{b}_\perp) \gamma^+ g F^{+i}(\mathbf{b}_\perp) q(\mathbf{b}_\perp) | \mathbf{R}_\perp = 0, p^+, \Lambda \rangle \\ &= |\mathcal{N}|^2 \int d^2\mathbf{p}_\perp \int d^2\mathbf{p}'_\perp \langle \mathbf{p}_\perp, p^+, \Lambda | \bar{q}(0) \gamma^+ g F^{+i}(0) q(0) | \mathbf{p}'_\perp, p^+, \Lambda \rangle e^{i\mathbf{b}_\perp \cdot (\mathbf{p}_\perp - \mathbf{p}'_\perp)} \end{aligned}$$

↔ determine using x^2 moments of twist-3 GPDs

- polarized quarks $\gamma^+ \rightarrow \gamma^+ \gamma_5, i\sigma^{+\perp}$

$$\begin{aligned} \langle p', \lambda' | \bar{q}(0) \gamma^+ i g F^{+i}(0) q(0) | p, \lambda \rangle &= \bar{u}(p', \lambda') \left[\frac{P^+}{M} \gamma^+ \frac{\Delta^i}{M} F_{FT,1}(t) + \frac{P^+}{M} i\sigma^{+i} F_{FT,2}(t) \right. \\ &\quad \left. + \frac{P^+}{M} \frac{\Delta^i}{M} \frac{i\sigma^{+\Delta}}{M} F_{FT,3}(t) + \frac{P^+}{M} \frac{\Delta^+}{M} \frac{i\sigma^{i\Delta}}{M} F_{FT,4}(t) \right] u(p, \lambda) \end{aligned}$$

- $F_{FT,i}(t) \leftrightarrow x^2$ moment of twist-3 GPDs

⊥ force distribution (unpolarized quarks)

$$\begin{aligned}
 F_{\Lambda'\Lambda}^i(\mathbf{b}_\perp) &\equiv \langle \mathbf{R}_\perp = 0, p^+, \Lambda' | \bar{q}(\mathbf{b}_\perp) \gamma^+ g F^{+i}(\mathbf{b}_\perp) q(\mathbf{b}_\perp) | \mathbf{R}_\perp = 0, p^+, \Lambda \rangle \\
 &= |\mathcal{N}|^2 \int d^2 \mathbf{p}_\perp \int d^2 \mathbf{p}'_\perp \langle \mathbf{p}_\perp, p^+, \Lambda | \bar{q}(0) \gamma^+ g F^{+i}(0) q(0) | \mathbf{p}'_\perp, p^+, \Lambda \rangle e^{i\mathbf{b}_\perp \cdot (\mathbf{p}_\perp - \mathbf{p}'_\perp)}
 \end{aligned}$$

$$\begin{aligned}
 \langle p', \lambda' | \bar{q}(0) \gamma^+ i g F^{+i}(0) q(0) | p, \lambda \rangle &= \bar{u}(p', \lambda') \left[\frac{P^+}{M} \gamma^+ \frac{\Delta^i}{M} F_{FT,1}(t) + \frac{P^+}{M} i \sigma^{+i} F_{FT,2}(t) \right. \\
 &\quad \left. + \frac{P^+}{M} \frac{\Delta^i}{M} \frac{i \sigma^{+\Delta}}{M} F_{FT,3}(t) + \frac{P^+}{M} \frac{\Delta^+}{M} \frac{i \sigma^{i\Delta}}{M} F_{FT,4}(t) \right] u(p, \lambda)
 \end{aligned}$$

$F_{FT,3}$

- tensor type force
- similar to charged particle flying through magnetic dipole field

$F_{FT,4}$

- no contribution for $\Delta^+ = 0$

⊥ force distribution (unpolarized quarks)

$$\begin{aligned}
 F_{\Lambda'\Lambda}^i(\mathbf{b}_\perp) &\equiv \langle \mathbf{R}_\perp = 0, p^+, \Lambda' | \bar{q}(\mathbf{b}_\perp) \gamma^+ g F^{+i}(\mathbf{b}_\perp) q(\mathbf{b}_\perp) | \mathbf{R}_\perp = 0, p^+, \Lambda \rangle \\
 &= |\mathcal{N}|^2 \int d^2 \mathbf{p}_\perp \int d^2 \mathbf{p}'_\perp \langle \mathbf{p}_\perp, p^+, \Lambda | \bar{q}(0) \gamma^+ g F^{+i}(0) q(0) | \mathbf{p}'_\perp, p^+, \Lambda \rangle e^{i\mathbf{b}_\perp \cdot (\mathbf{p}_\perp - \mathbf{p}'_\perp)}
 \end{aligned}$$

$$\begin{aligned}
 \langle p', \lambda' | \bar{q}(0) \gamma^+ i g F^{+i}(0) q(0) | p, \lambda \rangle &= \bar{u}(p', \lambda') \left[\frac{P^+}{M} \gamma^+ \frac{\Delta^i}{M} F_{FT,1}(t) + \frac{P^+}{M} i \sigma^{+i} F_{FT,2}(t) \right. \\
 &\quad \left. + \frac{P^+}{M} \frac{\Delta^i}{M} \frac{i \sigma^{+\Delta}}{M} F_{FT,3}(t) + \frac{P^+}{M} \frac{\Delta^+}{M} \frac{i \sigma^{i\Delta}}{M} F_{FT,4}(t) \right] u(p, \lambda)
 \end{aligned}$$

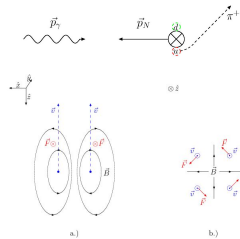
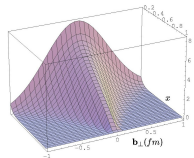
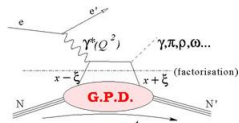
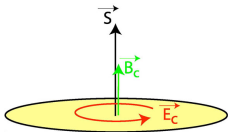
$F_{FT,1}$

- unpolarized target
- axially symmetric 'radial' force

$F_{FT,2}$

- ⊥ polarized target; force ⊥ to target spin
- ↪ spatially resolved Sivers force

- GPDs $\xrightarrow{FT} q(x, \mathbf{b}_\perp)$ '3d imaging'
- x^2 moment of twist-3 PDFs \rightarrow force
- x^2 moment of twist-3 GPDs
- $\hookrightarrow \bar{q}\gamma^+ F^{+\perp} \Gamma q$ distribution
- $\hookrightarrow \perp$ force tomography



- GPDs $\xrightarrow{FT} q(x, \mathbf{b}_\perp)$ '3d imaging'
 - x^2 moment of twist-3 PDFs \rightarrow force
 - x^2 moment of twist-3 GPDs
- $\hookrightarrow \bar{q}\gamma^+ F^{+\perp} \Gamma q$ distribution
- $\hookrightarrow \perp$ force tomography

